CRACK GROWTH AND LIFETIME OF CONCRETE UNDER LONG TIME LOADING

By Zdeněk P. Bažant,[1] Fellow, ASCE, and Yuyin Xiang[2]

ABSTRACT: Edge-notched eccentrically compressed fracture specimens made of aggregate of reduced size are loaded in standard creep test frames. Measurements of the time rate of crack mouth opening in notched concrete specimens subjected to constant load of almost one month duration are reported and analyzed. To reveal the size effect, geometrically similar specimens of four sizes in the ratio 1:2:4:8 are tested. The results are successfully described by a previously proposed time-dependent generalization of the R-curve model, in which the rate of crack growth is a function of the ratio of the stress intensity factor to the R-curve, and linear aging viscoelastic creep in the bulk of the specimen is treated according to the operator method. Good predictions are also obtained with a simplified method in which the R-curve is replaced by a constant asymptotic value of the critical stress intensity factor and creep is handled in similarity to the effective modulus method, neglecting the history effect. The time curves of crack opening terminate with an infinite slope, indicating the lifetime. The finiteness of the lifetime is not caused by creep, but by time-dependent crack growth, which dominates the final stage of crack opening. The initial stage of crack opening, on the other hand, is dominated by creep. Tests are conducted both for concretes of normal strength of 33.4 MPa (4,847 psi) in compression and relatively high strength of 46.4 MPa (6,442 psi). For the stronger concrete, the lifetimes are found to be longer. An increase of specimen size is found to decrease the lifetime. Since the same type of model was previously shown capable of describing all other known time-dependent fracture phenomena in concrete, a rather general applicability may be expected.

INTRODUCTION

During the last several decades, the time dependence of fracture and damage has been of key interest for many materials, including concrete, and much has been learned about the influence of the rate of loading [e.g., Shah and Chandra (1970); Wittmann and Zaistev (1972); Hughes and Watson (1978); Bažant and Oh (1982); Mindess (1985); Reinhardt (1985); Wittmann (1985); Darwin and Attiogbe (1986); Liu et al. (1989); Ross and Kuennen (1989); Harsh et al. (1990); Bažant and Jirásek (1993)]. However, most previous studies were limited in various respects. They were focused mainly on the loading rate effect on fracture in the dynamic range. In the static range, this effect was recently studied experimentally by Bažant and Gettu (1992) for concrete and by Bažant et al. (1993) for rock, with loading duration ranging from 1 s to almost three days.

The modeling of rate effect in the static range is in one respect easier than in the dynamic range, because the inertia effects and the wave propagation effects need not be considered, but in another respect it is more difficult, because creep phenomena in the bulk of material become significant. Understanding of the effect of loading rate and load duration of many years is important for many concrete structures, for example dams. The fracture parameters governing the slow growth of cracking in dams, which take many years to develop, are very different from the fracture parameters governing the additional rapid crack growth under an earthquake.

For quasi-brittle materials such as concrete, the modeling of fracture, including its time-dependent aspects, is complicated by the existence of a large fracture process zone. This causes a size effect representing a transition from plasticity-like behavior for small sizes to linear elastic fracture mechanics (LEFM) for large sizes. The size effect aspect of fracture, which is important for practical applications, has been studied extensively during the last decade [e.g., Bažant (1984); Bažant and Kazemi (1990); Bažant (1995)].

The size effect needs to be taken into account in studies of rate and time dependence of fracture. Conversely, the size effect plot, that is, the plot of the nominal strength of structure versus the characteristic structure size, must be considered to depend on the loading rate or duration. This effect was experimentally explored and quantified by Bažant and Gettu (1989, 1992) and Bažant et al. (1993). These studies revealed that the loading rate significantly influences the brittleness of concrete, but not of rock, the brittleness being understood as the proximity of the response to LEFM (with changes of brittleness being manifested by horizontal shift of the size effect plot toward LEFM). In Bažant et al. (1993), the influence of the loading rate on the size effect has been approximately described by quasi-elastic analysis, in which the behavior at each loading rate for different specimen sizes is tested according to time-independent LEFM using an elastic modulus that in effect represents the well-known effective modulus for creep. Such a simplification is practically valuable but cannot be used in a general model, since it cannot distinguish among different loading histories.

The effect of a sudden change in the loading rate in the static range was experimentally studied by Bažant et al. (1995) and Tandon et al. (in press 1997). These studies revealed a new phenomenon, namely a reversal of softening to hardening when the loading rate is increased suddenly. The test results on static fracture of specimens of various sizes loaded at different rates or with a sudden change of loading rate were successfully described by Bažant and Jirásek (1993) by an extension of the R-curve model. The rate of crack length increase was assumed proportional to a power function of the ratio of the stress intensity factor to its critical value given by the R-curve, and the creep in the bulk of the specimen was considered according to linear viscoelasticity.

A more fundamental model of these phenomena, consisting of an extension of the cohesive (fictitious) crack model for concrete originally proposed by Hillerborg (1976) as an adaptation of Barenblatt's (1959) model, has recently been presented by Bažant (1983), Wu and Bažant (1993), Bažant and Li (1996), and Li and Bažant (1996). In those studies, the activation energy theory was used to formulate a relationship between the cohesive (crack-bridging) stress and the crack opening displacement, and the operator method of linear vis-

[1]Walter P. Murphy Professor of Civil Engineering and Materials Science, Northwestern Univ., Evanston, IL 60208.

[2]Grad. Res. Asst., Northwestern Univ., Evanston, IL.

Note. Associate Editor: Robert Y. Liang. Discussion open until September 1, 1997. To extend the closing date one month, a written request must be filed with the ASCE Manager of Journals. The manuscript for this paper was submitted for review and possible publication on April 11, 1996. This paper is part of the ***Journal of Engineering Mechanics***, Vol. 123, No. 4, April, 1997. ©ASCE, ISSN 0733-9399/97/0004-0350–0358/ $4.00 + $.50 per page. Paper No. 13013.

coelasticity was applied to handle creep in the bulk of the structure. It was shown that the relaxation of support reaction of a cracked specimen as well as the shift of brittleness toward LEFM at a decreasing loading rate is caused by the viscoelasticity of the material, and that the reversal of softening to hardening at a sudden increase of loading rate is caused by the activation-energy–controlled process of bond ruptures. Also, crack face compliance functions were used to formulate an efficient numerical method for the time dependence of the cohesive crack model.

Although the law governing the time dependence of crack growth over a period of many years is of considerable practical interest, no tests of time dependence of fracture growth appear to have had durations exceeding three days. Also, no tests of crack growth in concrete under constant load seem to be available in the literature. This paper will report tests of crack growth at constant load for load duration up to almost one month. The tests involve concrete of normal as well as relatively high strength. The previously formulated time-dependent R-curve model (Bažant and Jirásek 1993) is adopted to model the results, and a method to calculate the lifetime of a structure based on time-dependent crack growth is presented.

TEST SPECIMENS AND PROCEDURE

The test specimens were eccentrically loaded fracture specimens of load eccentricities $e = D/8$ [Figs. 1(b,c)]. The reason for choosing a compression specimen is that this is the easiest specimen to subject to long-time loading. This kind of specimen can be loaded by means of the standard creep testing frames (which have already been available for this project). With other types of specimens, special loading frames would have to be built. (Loading by a testing machine over a very long period of time can hardly be afforded because it makes the testing machine unavailable for other projects.)

Two groups of specimens were cast, with one concrete of normal strength and another concrete of a relatively high strength [Fig. 1(a)]. The specimens were geometrically similar in two dimensions, with the same thickness $b = 76.2$ mm (3 in.). They were rectangular prisms of the same length-to-depth ratio, 8:3. The heights of the cross sections were $D = 38.1$, 76.2, 152.4, and 304.8 mm (or 1.5, 3, 6, and 12 in.). For each specimen size and each type of concrete, three specimens were cast, with a side of depth D in vertical position during casting. Two symmetrical notches of depth $D/6$ and thickness 2.5 mm (0.1 in.) were cut by a diamond saw when the specimens reached the age of 28 days [Figs. 1(a,c)].

The normal concrete was the same as that used by Bažant and Pfeiffer (1987), for which the fracture characteristics were determined in detail. The ratio of water, cement, sand, and gravel was 0.6:1:2:2 (by weight). The maximum aggregate size was $d_a = 12.7$ mm (0.5 in.) and the maximum grain size of sand was 12.8 mm (0.19 in.). Mineralogically, the aggregate consisted of crushed limestone and siliceous river sand. The aggregate and sand were air dried prior to mixing. Portland Cement 150, ASTM Type I, with no admixtures, was used.

For the concrete of higher strength, the ratio of water, cement, sand, and gravel was 0.35:1:1.4:2.4. Both a retarder (naphthalene based) and a high-range water reducer were used. The maximum aggregate size was again 12.7 mm (0.5 in.). Dundee Cement of ASTM Type I was used. The dosages by weight were 475 kg (1,047 lb) of cement, 641 kg (1,414 lb) of sand FA2, 1,152 kg (2,540 lb) of crushed limestone gravel CA15, 166 kg (366 lb) of water, 119 kg (272 lb) of fly ash Class C, 21 kg (46 lb) of microsilica (W.R. Grace Force 10,000), 1.31 L (46 oz) of naphthalene based retarder, and 6.9 L (236 oz) of high-range water reducer (Pozzolieth 100 XR) per cubic meter (1.31 cu yd) of concrete. To determine the strength, companion cylinders of diameter 76.2 mm (3 in.) and

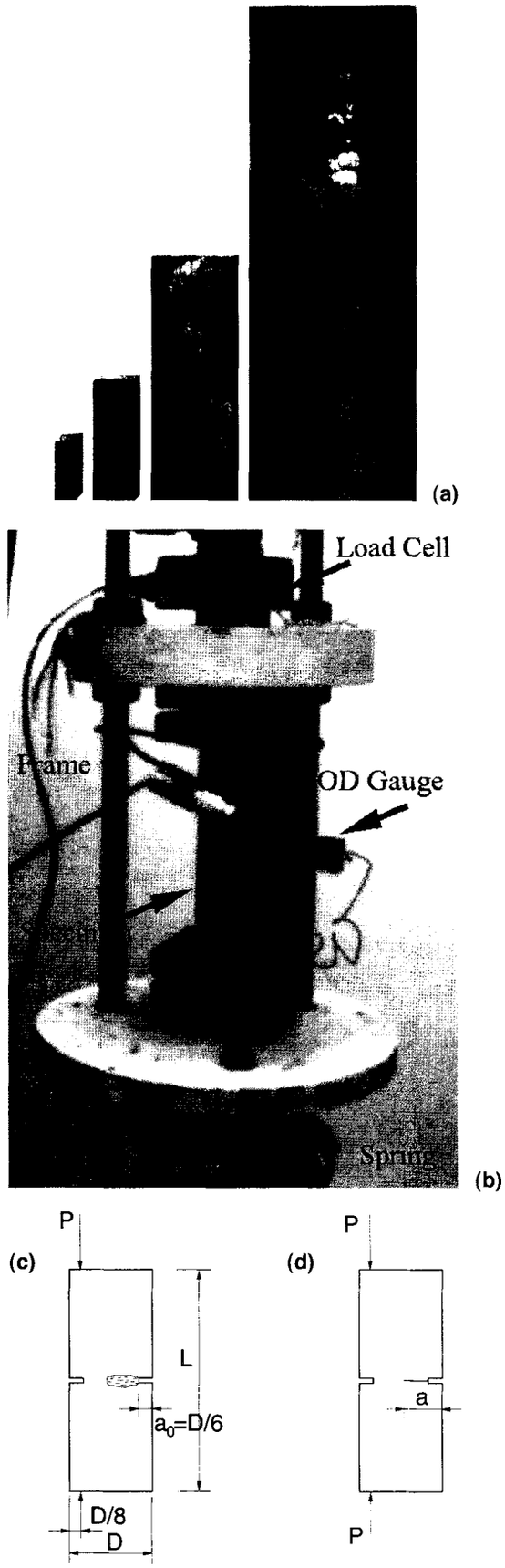

FIG. 1. Creep Specimens: (a) Edge-Notched Fracture Specimens Tested; (b) Instrumented Specimen in Loading Frame (d = 3 in.); (c) Eccentric Compression Loading and Fracture Process Zone; and (d) Equivalent Crack of Length a

height 152.4 mm (6 in.) were cast from concrete of each type. After the standard 28-d moist curing, the mean compression strength was $f_c' = 33.4$ MPa (4,847 psi) for normal concrete, with standard deviation 2.26 MPa (327 psi), and $f_c' = 44.4$ MPa (6,442 psi) for the higher strength concrete with standard deviation 3.05 MPa (442 psi). (The latter compression strength value is not enough for what is today called high-strength concrete.)

The specimens were cast in plywood forms and stripped one day after casting for the normal strength concrete, and two days after casting for the higher strength concrete. Subsequently the specimens were cured in water for 27 days at temperature 25°C (77°F). After that, the specimens were placed in a test chamber of relative humidity 50% and 25°C (77°F). One day before the test the specimens were sealed by silicon polymer. The ages of specimens at the start of the test were t_0 = 66, 31, 46, 80 (normal concrete, 50% of peak load); 99, 96, 93, 110 (normal concrete, 70% of peak load); 177, 172, 186, 179 (normal concrete, 90% of peak load); 549, 543, 573, 591 (concrete of higher strength, 70% of peak load); and 577, 561, 621, 630 (concrete of higher strength, 90% of peak load) days. The specimens under constant long-time load were tested in spring-loaded frames standardized by ASTM, as shown in Fig. 1(b). The spring constants of all the springs were 14 kN/m (800 lb/in.). One spring was used for the specimens of depth D = 38.1 and 76.2 mm (1.5 and 3 in.), and three springs were used for the specimens of D = 152.4 and 304.8 mm (6 and 12 in.).

For the concrete of normal strength, the applied loads under short-time loading were 50%, 70%, and 90% of the estimated short-time peak load. Because of the similarity of the concrete with that used before by Bažant and Pfeiffer (1987), it was possible to estimate the peak load using the size effect law $\sigma_N = Bf_t'[1 + (D/\lambda_0 d_a)]^{-1/2}$, in which σ_N = nominal strength of specimen = P/bD, P = peak load, b = specimen thickness, and B, λ_0 = two empirical constants, which are B = 1.239 and λ_0 = 4.561 according to the tests of Bažant and Pfeiffer. The tensile strength was estimated from the formula f_t'/MPa = $0.5\sqrt{f_c'}$/MPa (equivalent to f_t'/psi = $6\sqrt{f_c'}$/psi).

For the concrete of higher strength, there was no prior information, and so one specimen of each size had to be used to determine the short-time peak loads experimentally. This was done by a monotonic loading test of duration about 10 min, conducted in a servocontrolled closed-loop Materials Service Corporation (MTS) testing machine. The results of these short-time monotonic loading tests are shown in Fig. 2, along with an optimal fit by the size effect law. After determining the peak loads, the aforementioned size effect law was again applied to smooth out the results and thus suppress the test errors, which provided the estimates of the short-time peak loads. The remaining specimens were then tested under permanent loads representing 70% and 90% of the peak loads of the specimens for monotonic short-time loading.

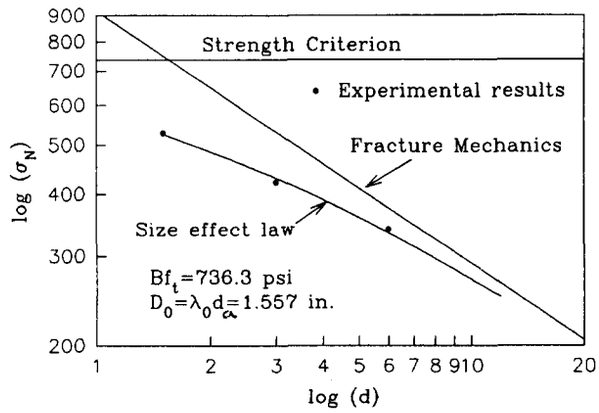

FIG. 2. Logarithmic Size Effect Plot Used to Smooth Out Predictions of Peak Loads under Monotonic Short-Time Loading

The specimens for the long-time tests in spring-loaded test frames were loaded by placing a jack at the top of the frame. The loading took about 15 min. The load was measured by a load cell. The springs were sufficiently soft to keep the load almost constant between any two readings. During the test, the crack mouth opening displacement Δ was measured by an inductive gauge. The readings were taken at the following times after the end of the initial loading procedure: 10 s, 20 s, 40 s, 1 min, 2 min, 4 min, 6 min, 10 min, 20 min, 40 min, 1 h, 2 h, 4 h, 6 h, 10 h, one day, and then every subsequent day. Before taking the readings, the load level was always checked by the load cell. Occasionally, when necessary, the load had to be slightly jacked up, and in that case the reading was taken 1 min after jacking.

TEST RESULTS AND TRENDS OBSERVED

The test results are reported in Fig. 3 for the concrete of normal strength and in Fig. 4 for the concrete of higher strength. The scales of time as well as crack mouth opening displacement (CMOD) are logarithmic. The test results are represented by the data points. The fits shown by the curves have been obtained by the theory explained later. As we see, initially the rate of CMOD tends to increase roughly as a power law of time (which corresponds to the initial straight line portions in Fig. 3), but later this rate progressively increases. In theory, it eventually approaches infinity, which means the lifetime is reached and the specimen breaks.

The recorded crack mouth openings Δ increase relatively smoothly for the specimens of normal strength (Fig. 3), but show occasional sudden jumps for the specimens of higher strength (Fig. 4). This phenomenon is probably caused by the

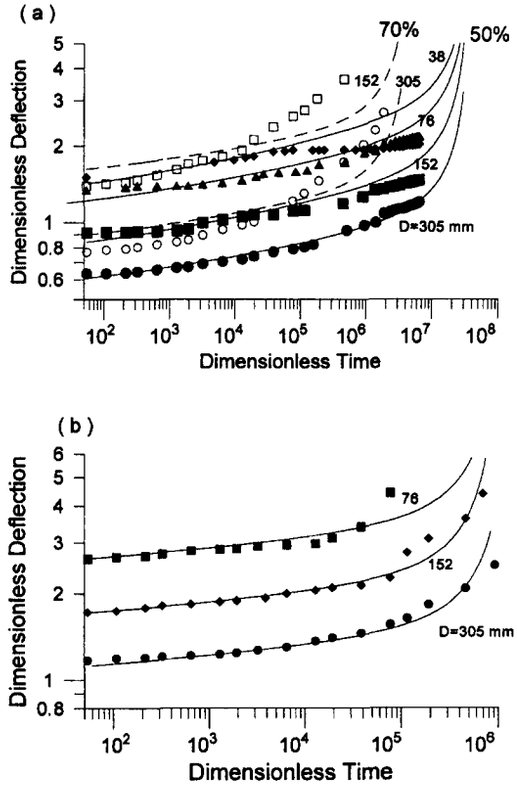

FIG. 3. Test Results for Specimen of Normal Strength of Different Sizes and Different Load Levels Compared with Calculated Time Curves of Crack Mouth Opening Displacement (CMOD): (a) 50% and 70% of Peak Load; (b) 90% of Peak Load

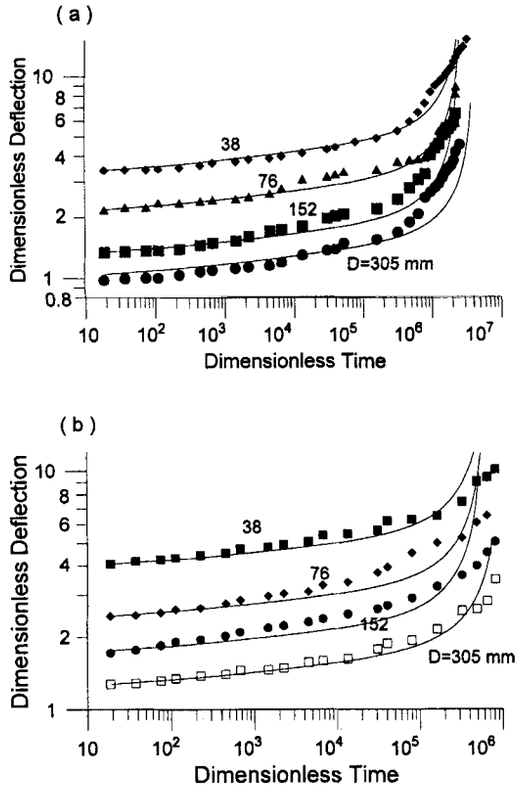

FIG. 4. Test Results for Specimens of Higher Strength, Various Load Levels, and Different Sizes Compared with Calculated Histories of Crack Mouth Opening Displacement: (a) 70% of Peak Load; (b) 90% of Peak Load

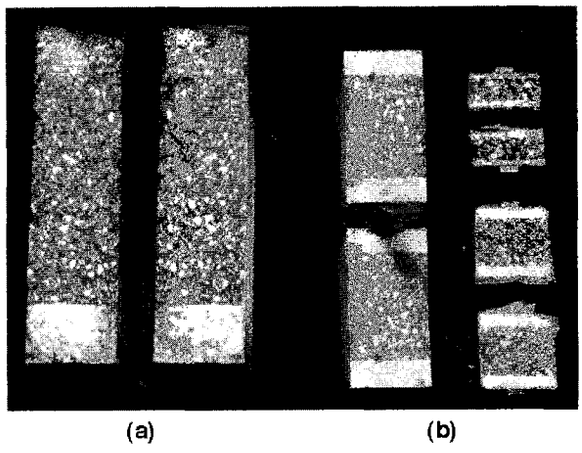

FIG. 5. Final Fracture Surfaces in Concrete of (a) Normal Strength and (b) Higher Strength

breaking of aggregate pieces in the concrete of higher strength. This is indicated by the pictures of the surface of the final break of the specimens (Fig. 5). In the concrete of higher strength, almost every aggregate piece on the crack surface is broken. The broken surfaces of the aggregates are seen as the white spots in Fig. 5(b) (located symmetrically on the surfaces). But in the normal strength concrete, there are only few such white spots. The black spots in Fig. 5(a) (which are not symmetrically located) are the aggregates.

Another phenomenon that can be noticed without any mathematical analysis is that the specimens of higher strength tend to have a longer lifetime than the specimens of normal strength [this is probably explained by a small value of the exponent in (6), to be discussed later].

MODELING BY TIME-DEPENDENT R-CURVE AND CREEP IN BULK

Fracture of quasi-brittle materials is nonlinear and can be modeled in three ways and with three levels of sophistication. The simplest model is to treat the fracture process zone as a point, using an adaptation of LEFM called the R-curve model. A more complicated but more realistic way is to treat the fracture process zone as a region of a finite but variable length and a fixed width, zero or finite. This is done in the cohesive (or fictitious) crack model as well as the crack band model. The most realistic but also difficult way to model fracture is to describe it as a two-dimensional region with distributed microcracking and other inelastic phenomena, as done approximately in nonlocal models of fracture. In this study, only the first approach, that is, the R-curve, is used, although the recently developed time-dependent formulation of the cohesive crack model based on crack face compliance function (Li and Bažant 1996) could also be used to describe the present data.

The R-curve model has been generalized for time dependence of crack growth and linear viscoelastic creep in the bulk material by Bažant and Jirásek (1993). That formulation is used to describe the present test results. For the reader's convenience, it is first briefly reviewed.

Denote a = total crack length from the mouth of the notch, $a_0 = D/6$ = initial crack length equal to the notch length, $\alpha = a/D$ = relative total crack length, and $\alpha_0 = a_0/D = 1/6$. The LEFM expressions for the CMOD Δ and the mode I stress intensity factor may be written in terms of dimensionless functions $k(\alpha)$ and $\delta(\alpha)$

$$\Delta = \frac{P}{E'b}\,\delta(\alpha); \quad K = \frac{P}{b\sqrt{D}}\,k(\alpha) \tag{1a,b}$$

Here P = applied load, $E' = E$ = Young's modulus for the case of plane stress, and $E' = E/(1 - \nu^2)$ for the case of plane strain. The dimensionless functions $\delta(\alpha)$ and $k(\alpha)$ characterize the structure or specimen geometry (its shape) but are independent of the structure size D. Although for many situations these functions are listed in handbooks, for the present fracture specimen they do not seem to be available. These functions have been determined by the finite element method, using a procedure called the domain integral method (Moran and Shih 1987), in which quarter-point quadrilateral elements (Barsoum 1976) were used around the crack tip to enforce the correct stress singularity. This method makes it possible to obtain rather accurate results. Computations with 800 eight-node isotropic elements and smoothing of the result by an analytical formula has led to the following expressions:

$$\delta(\alpha) = \left(\frac{5}{6} - \alpha\right)^{-3/2}(0.2815 + 4.456\alpha + 1.610\alpha^2 - 9.904\alpha^3 + 5.897\alpha^4) \tag{2}$$

$$k(\alpha) = \left(\frac{5}{6} - \alpha\right)^{-3/2}\sqrt{\pi\alpha}(1.566 - 4.738\alpha + 7.151\alpha^2 - 6.351\alpha^3 + 2.444\alpha^4) \tag{3}$$

In the R-curve approach, the critical value of the stress intensity factor K is not a constant but is assumed to depend on the crack extension $c = a - a_0$ according to a certain increasing function denoted $K_R(c)$. This function approximately reflects the gradual growth of the fracture process zone. Note that $K_R(c) = \sqrt{R(c)/E'}$, in which $R(c)$, called the resistance curve (R-curve), represents the critical energy release rate required for crack propagation. A convenient and, for the prediction of maximum loads, realistic way to determine $R(c)$ or $K_R(c)$ is through the knowledge of the size effect on the maximum loads of geometrically similar specimens. Based on the

size effect law, Bažant and Kazemi (1990) developed and Bažant and Jirásek (1993) used the formula

$$K_R(c) = K_f\sqrt{\rho(\alpha)} \tag{4}$$

in which

$$\rho(\alpha) = [g(\alpha) - (\alpha - \alpha_0)g'(\alpha)]/g(\alpha_0); \quad g(\alpha) = k^2(\alpha) \tag{5}$$

The R-curve depends on the specimen geometry, which is reflected in (4) and (5).

One important source of time dependence is a gradual breakage of bonds at the fracture front. In quasi-LEFM models such as the present R-curve model, this source of rate effect may be described as a dependence on the crack growth rate $\dot{a}$ on the applied stress intensity factor K (or the applied energy release rate). In similarity to a previous formulation for ceramics (Thouless et al. 1983; Evans and Fu 1984), and in view of certain arguments based on the activation energy theory (Bažant 1993, 1995), the following relation was proposed and justified by comparison with experiments (Bažant and Gettu 1992; He et al. 1992):

$$\dot{a} = \kappa\left(\frac{K}{K_R}\right)^q \tag{6}$$

where κ and q = empirical material constants. By using a very high value of exponent q, it is possible to reach agreement with the fact that a change of several orders of magnitude in the loading rate causes the peak load to change less than by a factor of 2.

The second important source of time dependence of fracture of concrete is the linear viscoelastic creep in the bulk material. The creep is characterized by compliance function $J(t, t_0)$, representing the strain in concrete at age t caused by a unit uniaxial stress acting since age t_0. For creep durations not exceeding several months, the compliance function of concrete can be very well described by the double power law [see, e.g., Bažant and Cedolin (1991), Sec. 9.4]

$$J(t, t') = \frac{1}{E_0}\{1 + \phi_1[t'^{-m} + \alpha_1(t - t')^n]\} \tag{7}$$

where ϕ_1, E_0, m, n, and α_1 = empirical constants whose typical values are ϕ_1 between 2 and 6, $E_0 \approx 1.5E$, $m \approx 1/3$, $n = 1/8$, and $\alpha_1 = 0.05$.

The problem is now described by (1) with (2) and (3); (4) with (5); (6); and (7). This is a system of differential equations that is highly nonlinear, but it can be integrated as follows (Bažant and Jirásek 1993). Eq. (6) provides the time increment as $dt = (D/\kappa)(K_R/K)^q\, d\alpha$, which achieves separation of variables t and α. Then, substituting (1b) and (4) into this equation and integrating, we obtain

$$\bar{t} = \frac{t(\alpha)}{\tau_f} = \bar{D}^{1-q/2}\int_{\alpha_0}^{\alpha}\left(\frac{f_t'\sqrt{\rho(\alpha')}}{\sigma_N k(\alpha')}\right)^q d\alpha' \tag{8}$$

with

$$\tau_f = \frac{l_f}{\kappa}; \quad \bar{D} = \frac{D}{l_f} = \frac{Df_t'^2}{K_f^2} \tag{9a,b}$$

where $\bar{t}$ = a dimensionless time parameter; f_t' = tensile strength of concrete, which is introduced only for the purpose of obtaining a dimensionless variable; τ_f = characteristic time; $\bar{D}$ = relative structure size; and $l_f = (K_f/f_t')^2$ = material length for fatigue fracture; l_f is similar but not identical to the material length $l_0 = K_c^2/f_t'$ for short-time monotonic fracture (representing Irwin's characteristic size of fracture process zone, called by Hillerborg the characteristic length).

The deflection at time t corresponding to α can be obtained by replacing $(1/E')$ in (1a) with the viscoelastic creep operator corresponding to (7). This yields

$$\Delta(t) = \frac{1}{b}\int_{t_0}^{t} J(t, t')\, d[P\delta(\alpha')] \tag{10}$$

This memory integral expresses the effect of load history. Substituting $P = bD\sigma_N$ and dividing the equation by D, we obtain the following expression for the dimensionless (relative) deflection corresponding to t at which the relative crack length is α:

$$\bar{\Delta}(t) = \frac{\Delta(t)}{D} = \int_{t_0}^{t} J[t(\alpha), t'(\alpha')]\, d[\sigma_N\delta(\alpha')] \tag{11}$$

Eqs. (8) and (11) are valid for time-dependent σ_N, although in the present test σ_N was constant [in which case σ_N can be brought in front of the integrals in (8) and (11)]. Eqs. (8) and (11) define the evolution of CMOD in time parametrically. We choose an increasing progression of α-values. For each of them, we can obtain the corresponding time by evaluating the integral in (8) and the corresponding CMOD by evaluating the integral in (11).

In (11) we assume all the parameters to be fixed except ϕ_1. Thus according to (8) and (11), the curve of $\bar{t}$ versus $\bar{\Delta}$ at constant σ_N depends only on three parameters, namely ϕ_1, τ_f, and q (in comparisons to the test data, one also needs to fix K_f, which can be estimated according to Bažant size effect law and LEFM).

For the purpose of numerical solution, we introduce discrete values α_i ($i = 0, 1, 2, 3, \ldots, N$). Because, for most of the test duration, the curve of $\alpha(t)$ is nearly straight in the logarithmic scale, it is best to choose the intervals (α_i, α_{i+1}) to be approximately constant in the logarithmic scale, that is, increasing as a power function. The subdivision $\alpha_i = (5/54) + (2/27)10^{i/N}$ has been used. It yields $\alpha_0 = 1/6$ and $\alpha_N = 5/6$, which agrees with the lengths of the notches in the present specimens. According to (8), the times t_{i+1} corresponding to α_{i+1} can be calculated by the recursive relation

$$\bar{t}_{i+1} = \bar{t}_i + \left(\frac{l_f}{D}\right)^{q/2-1}\left(\frac{f_t'\sqrt{\rho(\bar{\alpha})}}{\sigma_N k(\bar{\alpha})}\right)^q(\alpha_{i+1} - \alpha_i) \tag{12}$$

where $\bar{\alpha}$ stands for $(\alpha_i + \alpha_{i+1})/2$. Eq. (11) for CMOD can be numerically integrated as follows:

$$\bar{\Delta}_{i+1} = \sigma_N\sum_{j=0}^{i} J\left(t_{i+1}, \frac{t_j + t_{j+1}}{2}\right)[\delta(\alpha_{j+1}) - \delta(\alpha_j)] \tag{13}$$

COMPARISON OF THEORY TO EXPERIMENTAL RESULTS

To fit the test data presented here, the three parameters τ_f, q, and ϕ_1 are first varied in a trial-and-error fashion until a qualitative agreement is found. Subsequently it is best to use the Levenberg-Marquardt nonlinear optimization algorithm (a standard library subroutine) to optimize the parameter values by minimizing the sum of squares of the deviations from the data points. In simulating the test results, it is assumed that the creep during the initial process of applying the load, of duration about 15 min, is negligible. Thus, the initial CMOD is calculated directly from the LEFM formula [(1a)].

The optimal fits of the calculation results to the test data are shown by the continuous curve in Figs. 3 and 4. The optimized parameters for the optimal fits are for the concrete of normal stength: $\tau_f = 0.1842$ s, $q = 6.169$, and $\phi_1 = 3.335$, and for the concrete of higher strength: $\tau_f = 0.5311$ s, $q = 5.930$, and $\phi_1 = 4.190$. As can be seen, the calculation results agree with the test data reasonably well.

ANALYSIS OF TIME-DEPENDENT BEHAVIOR AND ITS SOURCES

A typical history of the relative crack length $\alpha = a/D$ is shown in Fig. 6(b), in conjunction with the corresponding CMOD history in Fig. 6(a). Fig. 7 shows typical calculated CMOD histories in the logarithmic and linear time scales, and illustrates how the history approaches a vertical asymptote representing the end of lifetime. Fig. 7 further shows the CMOD histories when only creep is taken into account, or when only the time-dependent crack growth is taken into account.

From these comparisons it becomes clear that the lifetime can approximately be divided into three stages. In stage 1, the CMOD increase is primarily governed by creep in the bulk of the specimen. In stage 2, both the creep and the time-dependent crack growth have a significant effect. In stage 3, the final one, the CMOD increase is primarily governed by the time-dependent crack growth. In that stage the CMOD rate approaches infinity, which means the end of lifetime. Further it is observed that the lifetime is governed mainly by the time dependence of crack growth. The lifetime is not significantly affected by creep because the vertical asymptotes that are approached by the curve for time-dependent crack growth only and by the curve for the combined effect with creep are found to be virtually the same.

Comparing Figs. 3 and 4, it further appears that the CMOD histories for the concrete of the higher strength have longer stages 1 and 2 and a shorter stage 3 than the CMOD histories for concrete of normal strength. Furthermore, it transpires from the comparison that the lifetime is longer for the concrete of higher strength. Actually, with τ_f and q known, one can easily evaluate $\kappa = 48.1$ mm/s (18.9 in./s) for the concrete of normal strength and 17.6 mm/s (6.95 in./s) for the concrete of higher strength. Because coefficient κ and exponent q in (6) are smaller, the specimens made of concrete of higher strength have a more prolonged stage II, which mainly determines the lifetime.

The experimentally observed lifetimes are listed for all the specimens in Table 1. Although the initial CMOD curves for specimens of the same concrete loaded to the same percentage

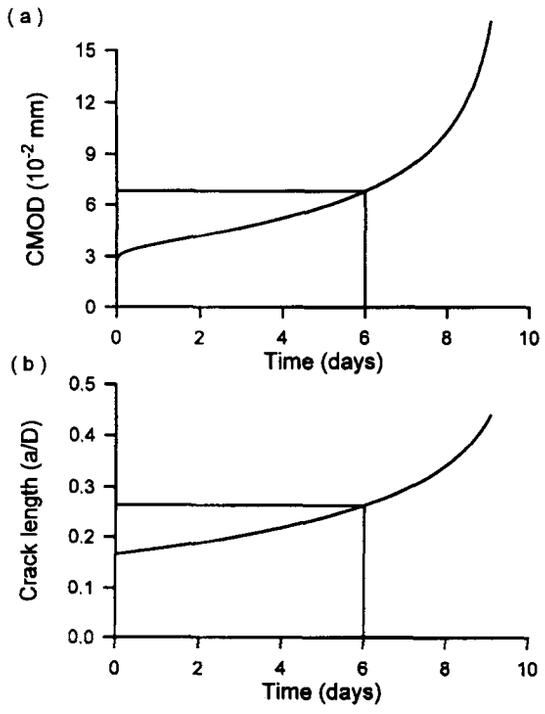

FIG. 6. Typical Histories of (a) CMOD; and (b) Crack Length

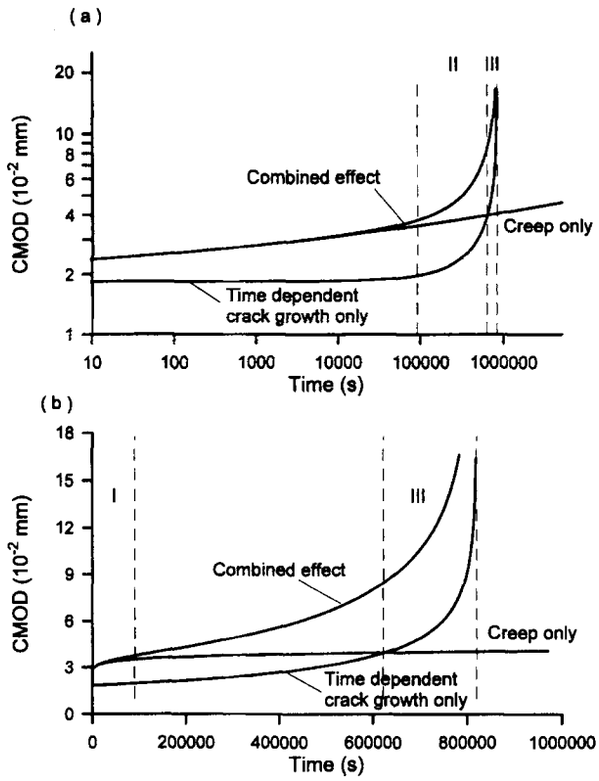

FIG. 7. Approach of CMOD Histories to Vertical Asymptote Representing Lifetime—Histories Obtained When either Creep or Time-Dependent Crack Growth Is Missing, and Stages in Each Different Mechanism Governing Growth: (a) Stage I, Logarithmic Scales; (b) Stage II, Linear Scale

TABLE 1. Lifetimes from Experiments and R-Curve

Specimen and load[a] (1)	Life Span (d) Experimental (2)	Life Span (d) Theoretical (3)
N3 × 1.5 × 4 50%	—	123
N3 × 3 × 8 50%	—	81
N3 × 6 × 16 50%	—	76
N3 × 12 × 32 50%	—	76
N3 × 1.5 × 4 70%	9	15
N3 × 3 × 8 70%	2	10
N3 × 6 × 16 70%	2	9.5
N3 × 12 × 32 70%	4.5	9.5
H3 × 1.5 × 4 90%	Failed during loading	3.3
N3 × 3 × 8 90%	0.21	2.3
N3 × 6 × 16 90%	2	2.2
N3 × 12 × 32 90%	3	2.1
H3 × 1.5 × 4 70%	22	18
H3 × 3 × 8 70%	14.21	17
H3 × 6 × 16 70%	17	16
H3 × 12 × 32 70%	28.13	16
H3 × 1.5 × 4 90%	9	4.9
H3 × 3 × 8 90%	14	4.7
H3 × 6 × 16 90%	7.21	4.6
H3 × 12 × 32 90%	7	4.6

Note: N, normal concrete; H, high-strength concrete.
[a]Percentage of peak load.

of the peak load are quite different, they tend to have about the same lifetime; for example, note the four specimens of higher strength concrete under 70% of their peak load, which all have failed between 14 and 21 days of loading despite rather different initial responses (the periods of 14 days and 21 days are quite close in the logarithmic time scale). Fig. 7 also provides visual evidence that the creep alone cannot cause

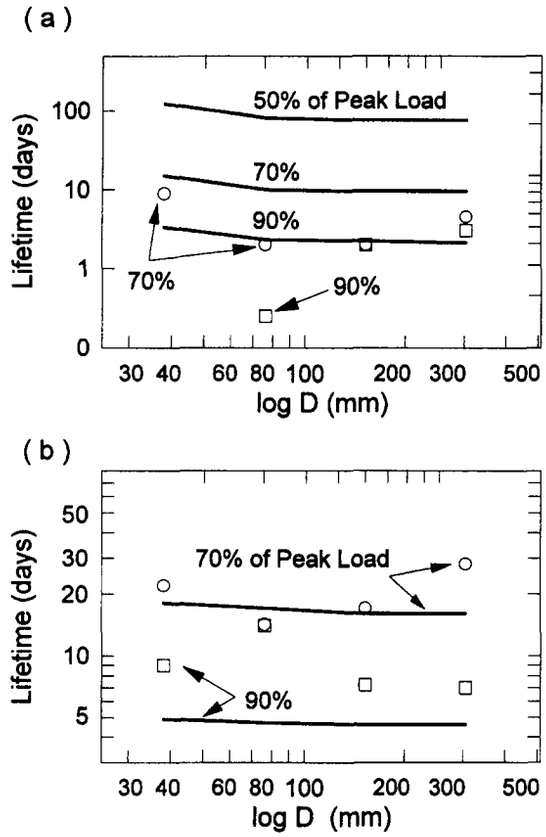

FIG. 8. Effect of Specimen Size on Lifetime of Concrete with (a) Normal Strength; and (b) Higher Strength

failure within a finite lifetime, but the time-dependent crack growth alone, without creep, can.

The calculated lifetimes in Table 1 are plotted in Fig. 8 as a function of specimen size D (solid lines), separately for various load levels and concrete types. The measured data points are also plotted. As we see, although there is a slight decrease of the calculated lifetimes with increasing size D, the decrease is negligible compared to the scatter of test results. One can conclude only that, for a given constant percentage of peak load for monotonic loading, the calculated lifetimes are approximately independent of specimen size D. The test data are highly scattered and do not disagree with this conclusion.

At the last ConCreep Conference in Barcelona, Spain (Bažant 1993), a provocative unorthodox proposition was made: The nonlinearity of concrete creep due to high stress is only apparent. In reality, nonlinear creep does not exist. Nonlinear creep really represents nothing but a manifestation of time-dependent growth of microcracks. The present findings tend to confirm this proposition. The crack opening increases with the load level in a highly nonlinear fashion, much faster than proportionally. This is due to the high value of exponent q in (12) [or in (16)], which tends to shorten the times corresponding to the linear portion of the deflection curve in (11). Function $\delta(\alpha)$ in (11) also contributes to this nonlinearity.

SIMPLIFIED SOLUTION NEGLECTING HISTORY EFFECT

As is well known from linear viscoelasticity, without or with aging, good solutions can often be obtained by using the effective modulus method in which the details of the stress history are neglected and its effect on creep is lumped into one parameter. The creep strain is calculated as if the creep-producing variable (which is stress) were constant in time and equal to its current value. According to (10), the creep-producing variable is here the product $\sigma_N\delta(\alpha)$, and the effective modulus is the inverse of $J(t, t_0)$. Therefore, in analogy with the effective modulus method, one may expect that the equation

$$\bar{\Delta} = \frac{\Delta(t)}{D} = \sigma_N J(t, t_0)\delta[\alpha(t)] \tag{14}$$

should give good estimates of the relative crack opening due to creep in the bulk of the specimen.

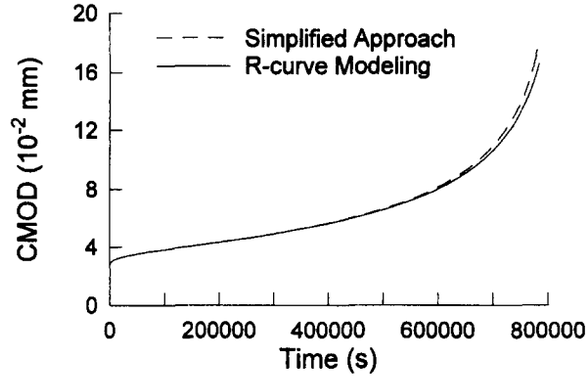

FIG. 9. CMOD Histories Obtained by Simplified Model (Dashed), Compared to History Obtained with Full Model (Solid)

As for the crack growth law, neglecting the effect of history essentially means neglecting the R-curve and taking the critical value of the stress intensity factor to be constant. For the lifetime, as already commented on, the rate of crack growth in the final stage of the test is most important. In the final stage, the crack has already grown significantly and the value of K_R must already have closely the approached K_f, the final critical stress intensity factor. Thus, omitting the history effect, the following relation appears appropriate:

$$\dot{a} = \kappa \left(\frac{K}{K_f}\right)^q \tag{15}$$

The foregoing approach greatly simplifies numerical solution, making it superfluous to evaluate the creep integrals over time. This reduces the programmer's effort and computer time. By discretizing (14) and (15) in the same manner as before, we get for the times corresponding to various crack lengths α_{i+1} the recursive relation

$$\bar{t}_{i+1} = \bar{t}_i + \left(\frac{l_f}{D}\right)^{q/2-1} \left(\frac{f_t'}{\sigma_N k(\bar{\alpha})}\right)^q (\alpha_{i+1} - \alpha_i) \tag{16}$$

The corresponding CMOD, according to (14), then is

$$\bar{\Delta}_{i+1} = \sigma_N J(t_{i+1}, t_0)\delta(\alpha_{i+1}) \tag{17}$$

This simplified solution is shown in Fig. 9 by the dashed curve for one typical case of response. The exact solution according to the present model with R-curve and a memory-type creep law is shown by the solid curve. The two solutions are seen to be extremely close. Thus, for practical purposes, the simplified solution that neglects the history effect is sufficient. In fact, it is even on the safe side, giving a slightly shorter lifetime than the exact solution.

Like the preceding accurate solution, the simplified solution shows that the lifetime depends on both the crack growth law and the law of creep.

CONCLUSIONS

1. The effect of long-time loading on fracture growth in concrete can be effectively measured on edged-notched eccentrically loaded compression fracture specimens, using the same loading frames as for long-time compression creep tests.

2. The time-dependent fracture model developed previously (Bažant and Jirásek 1993) was verified by test data up to only three days of duration, which included constant displacement rate tests, tests with a sudden change of displacement rate, and stress relaxation tests. The present test results confirm that this model can also successfully describe time-dependent fracture behavior up to about one month duration. There are two essential aspects of the model: (1) a power law relating the crack growth rate to the applied stress intensity factor; and (2) a linearly viscoelastic creep in the bulk of the structure. The crack growth model is properly formulated as a generalization of the R-curve model.

3. The description of the test results for sustained load does not get significantly worse if one uses a simplified model in which creep is handled in the sense of the effective modulus, neglecting the effect of variable stress history, and the R-curve is replaced by a constant critical stress intensity factor equal to the final value of the R-curve.

4. The time curve of crack mouth opening displacement can be subdivided into three stages. In the first stage, in which the rate of crack opening is decreasing with time, the response is governed mainly by viscoelastic behavior in the bulk. In the second stage, the time-dependent crack growth law becomes also important. The third stage, which leads to an infinite opening rate (failure, end of lifetime), is dominated by the time-dependent crack growth law reflecting the rate of bond breakages, while the creep becomes unimportant.

5. For a material without creep (e.g., rocks or ceramics), the theory also predicts a finite lifetime. But for a hypothetical material without time-dependent crack growth, the lifetime would be predicted as infinite.

6. In a concrete of higher strength, the stage dominated by creep lasts longer and the time-dependent crack growth is manifested later. This causes that, for the same ratio of the applied load to the peak load at short-time monotonic loading, the specimens of the stronger concrete have a longer lifetime.

7. Although the lifetime, as calculated for geometrically similar specimens of different sizes loaded to the same percentage of the monotonic peak load, slightly decreases with increasing size, this effect is hardly discernible from the test results, due to scatter. Approximately, the same load ratio means about the same lifetime, regardless of structure size.

8. The measured time curves of crack mouth opening displacement are relatively smooth for concrete of normal strength but exhibit sudden jumps for concrete of higher strengths. These jumps may be explained by the fact that, in a concrete of high strength, the crack tends to cut in sudden jumps through the aggregate pieces rather than pass around them.

ACKNOWLEDGMENTS

Partial financial support under NSF Grant MSS-9114426 to Northwestern University is gratefully acknowledged. Thanks are due to Jaime Moreno for arranging the production of the test specimens of higher strength concrete in his laboratory of the Materials Service Corp., in Chicago. Further thanks are due to Zhisheng Wu, of Ibaraki University, Tokyo, and a visiting scholar at Northwestern University, for his valuable comments and discussions. Finally, thanks are due to Laura Kazan, a student at Case Western University and visiting NSF trainee at Northwestern University, for her dilligent assistance in the conduct of experiments and some calculations.

APPENDIX. REFERENCES

Barenblatt, G. I. (1959). "The formation of equilibrium cracks during brittle fracture—general ideas and hypothesis, axially symmetric cracks." *Prikl. Math. Mekh.*, 23(3), 434–444.

Barsoum, R. (1976). "On the use of isotropic finite elements in linear fracture mechanics." *Int. J. Numer. Methods in Engrg.*, 10, 25–37.

Bažant, Z. P. (1995). "Creep and damage in concrete." *Materials Science of Concrete IV*, J. Skalny and S. Mindess, eds., Am. Ceramic. Soc., Westerville, Ohio, 355–389.

Bažant, Z. P. (1983). "Fracture in concrete and reinforced concrete." *Preprint, IUTAM Prager Symp. on Mech. of Geomat.: Rocks, Concrete, Soil*, Z. P. Bažant, ed., Int. Union on Theoretical and Appl. Mech., 281–316.

Bažant, Z. P. (1984). "Size effect in blunt fracture: Concrete, rock and metal." *J. Engrg. Mech.*, ASCE, 110(4), 518–535.

Bažant, Z. P. (1993). "Current status and advances in the theory of creep and interaction with fracture." *Proc., 5th Int. RILEM Symp. on Creep and Shrinkage of Concrete (ConCreep 5)*, Z. P. Bažant and I. Carol, eds., E & FN Spon, London, U.K., 291–307.

Bažant, Z. P., Bai, S.-P., and Gettu, R. (1993). "Fracture of rock: Effect of loading rate." *Engrg. Fracture Mech.*, 45(3), 393–398.

Bažant, Z. P., and Cedolin, L. (1991). *Stability of structures: Elastic, inelastic, fracture and damage theories*. Oxford University Press, New York, N.Y.

Bažant, Z. P., and Gettu, R. (1989). "Determination of nonlinear fracture characteristics and time dependence from size effect." *Fracture of concrete and rock: Recent developments*, S. P. Shah, S. E. Swartz, and B. Barr, eds., Elsevier, London, U.K., 549–565.

Bažant, Z. P., and Gettu, R. (1992). "Rate effects and load relaxation in static fracture of concrete." *ACI Mat. J.*, 89(Sept.), 456–467.

Bažant, Z. P., Gu, W.-H., and Faber, K. T. (1995). "Softening reversal and other effects of a change in loading rate on fracture of concrete." *ACI Mat. J.*, 92, 3–9.

Bažant, Z. P., and Jirásek, M. (1993). "R-curve modeling of rate and size effects in quasibrittle fracture." *Int. J. Fracture*, 62, 355–373.

Bažant, Z. P., and Kazemi, M. T. (1990). "Determination of fracture energy, process zone length and brittleness number from size effect, with application to rock and concrete." *Int. J. Fracture*, 44, 111–131.

Bažant, Z. P., and Li, Y.-N. (1995a). "Stability of cohesive crack model: Part I—Energy principles." *J. Appl. Mech.*, 62(Dec.), 959–964.

Bažant, Z. P., and Li, Y.-N. (1995b). "Stability of cohesive crack model: Part II—Eigenvalue analysis of size effect on strength and ductility of structures." *J. Appl. Mech.*, 62(Dec.), 965–969.

Bažant, Z. P., and Li, Y.-N. (1996). "Cohesive crack model with rate-dependent opening and viscoelasticity." *Rep.*, Dept. of Civ. Engrg., Northwestern Univ., Evanston (submitted to *Int. J. of Fracture*).

Bažant, Z. P., and Oh, B.-H. (1982). "Strain-rate effect in rapid triaxial loading of concrete." *J. Engrg. Mech. Div.*, ASCE, 108(5), 764–782.

Bažant, Z. P., and Pfeiffer, P. A. (1987). "Determination of fracture energy from size effect and brittleness number." *ACI Mat. J.*, 84(6), 463–480.

Darwin, D., and Attiogbe, E. K. (1986). "Effects of loading rate on cracking of cement paste in compression." *Cement based composites: Strain rate effects on fracture*, S. Mindess and S. P. Shah, eds., 167–180.

Evans, A. G., and Fu, Y. (1984). "The mechanical behavior of alumina." *Fracture of ceramic materials*, Noyes Publications, Park Ridge, N.J., 56–88.

Harsh, S., Shen, Z., and Darwin, D. (1990). "Strain-rate sensitive behavior of cement paste and mortar in compression." *ACI Mat. J.*, 87(5), 508–516.

He, S., Plesha, M. E., Rowlands, R. E., and Bažant, Z. P. (1992). "Fracture energy tests of dam concrete with rate and size effects." *Dam Engrg.*, 3(2), 139–159.

Hillerborg, A., Modéer, M., and Peterson, P. E. (1976). "Analysis of crack formation and crack growth in concrete by means of fracture mechanics and finite elements." *Cement and Concrete Res.*, 6, 773–782.

Hughes, B. P., and Watson, A. J. (1978). "Compressive strength ultimate strain of concrete under impact loading." *Magazine of Concrete Res.*, 30, 189–199.

Li, Y.-N., and Bažant, Z. P. (1994). "Eigenvalue analysis of size effect for cohesive crack model." *Int. J. Fracture*, 66, 213–226.

Liu, Z.-G., Swartz, S. E., Hu, K. K., and Kan, Y.-C. (1989). "Time dependent response and fracture of plain concrete beam." *Fracture of concrete and rock: Recent developments*, S. P. Shah, S. E. Swartz, and B. Barr, eds., Elsevier, London, U.K., 577–586.

Mindess, S. (1985). "Rate of loading effects on the fracture of cementitious materials." *Application of fracture mechanics to cementitious composites*, S. P. Shah, ed., Martinus Nijhoff Publishers, Dordrecht, The Netherlands, 617–638.

Moran, B., and Shih, C. F. (1987). "Crack tip and associated domain integrals from momentum and energy balance." *Engrg. Fracture Mech.*, 27, 615–642.

Neville, A. M., Dilger, W. H., and Brooks, J. J. (1983). *Creep of plain and structural concrete*. Construction Press, London, U.K.

Reinhardt, H. W. (1985). "Tensile fracture of concrete at high rates of loading." *Application of fracture mechanics to cementitious compos-*

ites, S. P. Shah, ed., Martinus Nijhoff Publishers, Dordrecht, The Netherlands, 559–592.
Ross, C. A., and Kuennen, S. T. (1989). "Fracture of concrete at high strain rates." *Fracture of concrete and rock: Recent developments*, S. P. Shah, S. E. Swartz, and B. Barr, eds., Elsevier, London, U.K., 152–161.
Shah, S. P., and Chandra, S. (1970). "Fracture of concrete subjected to cyclic and sustained loading." *Am. Concrete Inst., J.*, 67, 816–825.
Tandon, S., Faber, K. T., Bažant, Z. P., and Li, Y.-N. (1997). "Cohesive crack modeling of influence of sudden changes in loading rate on concrete fracture." *Engrg. Fracture Mech.*, in press.
Thouless, M. D., Hsueh, C. H., and Evans, A. G. (1983). "A damage model of creep crack growth in polycrystals." *Acta Metallurgica*, 31(10), 1675–1687.
Wittman, F. H. (1985). "Influence of time on crack formation and failure of concrete." *Application of fracture mechanics to cementitious composites*, S. P. Shah, ed., Martinus Nijhoff Publishers, Dordrecht, The Netherlands, 593–616.
Wittmann, F. H., and Zaitsev, Y. (1972). "Behavior of hardened element paste and concrete under high sustained load." *Mechanical Behavior of Mat., Proc., 1971 Int. Conf. Soc. of Mat. Sci.*, Japan, 84–95.
Wu, Z.-S., and Bažant, Z. P. (1993). "Finite element modeling of rate effect in concrete fracture with influence of creep." *Proc., 5th Int. RILEM Symp. on Creep and Shrinkage of Concrete*, Z. P. Bažant and I. Carol, eds., E & FN Spon, London, U.K., 427–432.